PROCEEDINGS OF SPIE

SPIEDigitalLibrary.org/conference-proceedings-of-spie

Radio link design framework for WSN deployment and performance prediction

Sergio Saponara, Filippo Giannetti

Sergio Saponara, Filippo Giannetti, "Radio link design framework for WSN deployment and performance prediction," Proc. SPIE 10246, Smart Sensors, Actuators, and MEMS VIII, 102461J (30 May 2017); doi: 10.1117/12.2265312

SPIE.

Event: SPIE Microtechnologies, 2017, Barcelona, Spain

Radio Link Design Framework for WSN Deployment and Performance Prediction

Sergio Saponara, Filippo Giannetti
Dip. Ingegneria della Informazione, Università di Pisa, via G. Caruso 16, 56122, Pisa, Italy

ABSTRACT

For an easy implementation of wireless sensor and actuator networks (WSAN), the state-of-the-art is offering single-chip solutions embedding in the same device a microcontroller core with a wireless transceiver. These internet-on-chip devices support different protocols (Bluetooth, ZigBee, Bluetooth Low Energy, sub- GHz links), from about 300 MHz to 6 GHz, with max. sustained bit-rates from 250 kb/s (sub-GHz links) to 4 Mb/s (Wi-Fi), and different trade-offs between RX sensitivity (from -74 to -100 dBm), RX noise figure (few dB to 10 dB), maximum TX power (from 0 to 22 dBm), link distances, power consumption levels (from few mW to several hundreds of mW). One limit for their successful application is the missing of an easy-to-use modeling and simulation environment to plan their deployment. The need is to predict, before installing a network, at which distances the sensors can be deployed, the real achievable bit-rate, communication latency, outage probability, power consumption, battery duration. To this aim, this paper presents the H^2AWKS (Harsh environment and Hardware Aware Wireless linK Simulator) simulator, which allows the planning of a WSAN taking into account environment constraints and hardware parameters. Applications of H^2AWKS to real WSAN case studies prove that it is an easy to use simulation environment, which allows design exploration of the system performance of a WSAN as a function of the operating environment and of the hardware parameters of the used devices.

Keywords: wireless sensor and actuator networks (WSAN), harsh environment, network simulations, internet-on-chip

1. INTRODUCTION

To address the needs of Cyber Physical System applications, and particularly for an easy implementation of wireless sensor and actuator networks (WSAN), semiconductor companies are offering single-chip solutions embedding in the same device a microcontroller core with a wireless transceiver. These *internet-on-chip* devices are available as COTS (Components Off The Shelf). These devices support different types of connections [1-4]: Bluetooth, ZigBee and Bluetooth Low Energy at 2.4 GHz, Wi-Fi at 2.4 or 5 GHz, sub-GHz ISM (Industrial, Scientific, Medical) at 868/915 MHz or 315/433 MHz. The used microcontroller cores range from 8-bit 8051 for low-power short-range solutions to 32-bit Cortex-M ARM ones. The max. sustained bit-rates are from tens of kb/s (sub-GHz links) to 54 Mb/s (Wi-Fi). At the state of the art there are different trade-offs between receiver sensitivity (from -74 dBm to -111 dBm) and maximum transmitter power (from - 5 dBm to 20 dBm). These performance parameters lead to different link distances, but also to different power consumption levels, from few mW to several hundreds of mW. A range extender device can be added [5] to improve RX noise figure (down to 4.7 dB) and TX power (up to 22 dBm), although for a power overhead of 480 mW.
Although a large set of embedded devices for WSANs exist, a severe limit for their application is the lack of an easy-to-use modeling and design framework for planning their deployment. The need is to predict, before installing a network, at which distances the sensors can be deployed, the real achievable bit-rate, the real communication latency, the outage probability, the power consumption (and hence battery duration).
To this aim, we have developed the H^2AWKS (Harsh environment and Hardware Aware Wireless linK Simulator) environment, which allows the planning of a WSAN taking into account: 1) environment constraints, e.g. target Bit Error Rate (*BER*), presence of time-dispersive and frequency-selective channels, shadowing and occlusion, propagation losses with/without line-of-sight (LOS/NLOS), single or multi hop, outdoor or indoor, in presence of interference sources in the same band; 2) hardware parameters, e.g. RX noise figure and sensitivity, TX power, operating frequencies, gains; 3) network parameters, e.g. network topology, modulation and channel coding scheme (MCS), packet size.
Hereafter, Section 2 reviews the wireless connection capability offered by internet-on-chip COTS devices. Section 3 discusses the set of models and equations used within H^2AWKS. Section 4 shows the simulation results using H^2AWKS. Conclusions are drawn in Section 5.

Smart Sensors, Actuators, and MEMS VIII, edited by Luis Fonseca, Mika Prunnila, Erwin Peiner, Proc. of SPIE
Vol. 10246, 102461J · © 2017 SPIE · CCC code: 0277-786X/17/$18 · doi: 10.1117/12.2265312

2. WIRELESS CONNECTION CAPABILITY OF INTERNET-ON-CHIP COTS DEVICES

Looking to the market of single-chip wireless transceivers lots of COTS solutions can be found by several vendors such as: Texas Instruments (TI), STMicroelectronics, Analog Devices, Linear Technologies, Maxim Integrated, to name just a few. The most diffused solutions are proposed for sub-GHz connections and for the spectrum portion from 2.4 GHz to 2.5 GHz where several standards operate: BT/BLE, ZigBee, Wi-Fi according to IEEE 802.11 b/g/n. Multi-standard chip are also available [6]. Most of these devices are designed to sustain a consumer temperature range (85 ^{0}C maximum) and for cost reasons they feature a plastic package, e.g. 64-pin QFN. Table 1 summarizes the characteristics of the most representative devices at the state of art.

For example, the CC3100 device from TI [7], sustaining around 2.4 GHz the IEEE 802.11 b/g/n, can achieve a maximum data-rate of 16 Mbps. This device feature a sensitivity of -95.7 dBm, using Direct Sequence Spread Spectrum (DSSS), and –74.0 dBm using Orthogonal Frequency-Division Multiplexing (OFDM), when considering a Packet Error Rate (PER) of 10% IEEE 802.11 g/n, 8% IEEE 802.11b. The transmitted output power is 18 dBm in DSS mode and 14.5 dBm in OFDM more. The current consumption is 0.7 mA in idle mode, 53 mA when receiving and up to 223 mA/272 mA when transmitting in DSSS/OFDM mode. In deep sleep mode the current consumption is 0.115 mA. The battery supply voltage should be from 2.1 V to 3.6 V (an internal 1.85 V voltage regulator is used). The RX saturation level is – 5 dBm. The CC3200 device has similar performance but integrates on-chip also a 32b Cortex M4 processor. Instead, the CC2564 [8] device supports around 2.4 GHz BT/BLE protocols, with max 3 Mbps data-rate. The transmitted power is up to 10 dBm, while the typical RX sensitivity is -93 dBm for a BER o 0.1% (- 85.5 dBm for a BER of 0.01 %). The RX saturation level is – 5 dBm.

ISM sub-GHz bands, with IEEE 802.15.4 protocol, are supported by the CC1310 device [9]. It has a RX sensitivity of – 124 dBm at 10 kbps with a BER of 10^{-2} in the 868 MHz and 915 MHz bands. The RX sensitivity is -110 dBm at 50 kbps. The TX power is programmable up to 14 dBm. The supply voltage range is 1.8 V to 3.8 V. The current consumption is 5.4 mA in RX mode and 13.4 mA in TX mode (at 10 dBm output power). The supported frequency bands are 315 MHz, 433 MHz, 470 MHz, 500 MHz, 779 MHz, 868 MHz, 915 MHz, 920 MHz. The SX1276 device [10] supports the LORA protocol. In Sub-GHz range can sustain up to 37.5 kbps with a RX sensitivity of -110 dBm. In case channel hopping is supported, the frequency synthetizer has a hop time of 50 µs for a frequency change of 50 MHz, 20 µs for a frequency change of 1 MHz. The MAX282x [11] device supports Wi-Fi at 2.4 GHz and 5 GHz (IEEE 802.11a/n/g). Finally, the HMC63xx [12] transceivers can support 60 GHz connections with a maximum TX power of 15 dBm, whereas the receiver has a NF of 8 dB, a gain of 67 dB and a maximum input power in linear range of -19 dB.

Table 1: Characteristics of the main wireless connectivity devices at the state of art

	Bit-rate max	RX sensitivity, dBm	RX saturation, dBm	TX power, dBm	Frequency range, GHz	Current consumption, mA	Standard
[7]	16 Mbps	-95.7@DSSS, -74 @OFDM	- 4	18 @DSSS, 14.5 @OFDM	2.4 to 2.5	53 RX, 272 DSSS/223 OFDM TX 0.7 idle	IEEE 802.11b/g/n
[8]	3 Mbps	-93	- 5	10	2.4 to 2.8	N/A RX, 112.5 TX 0.1 idle	BT/BLE
[9]	50 kbps	-110	N/A	10	Sub-GHz	5.4 RX, 13.4 TX	IEEE 802.15.4
[10]	37.5 kbps	-111	N/A	20	0.137-1.02	12 RX, 120 TX, 1.6 idle	LORA
[11]	54 Mbps	-74	N/A	-5	4.9 to 5.875	N/A	IEEE 802.11a/g/n
[12]	N/A	N/A	-19 dBm	15	57 to 64	N/A	IEEE 802.11 ad

3. SET OF MODELS AND EQUATIONS USED WITHIN H^{2}AWKS

In the following: "≡" means "by definition" and "~" denotes complex-valued variables. Also, given a bandpass random process $X(t)$, its power spectral density (PSD) is $S_X(f)$, its RF power is P_X and its baseband complex representation (BBCR) is $\tilde{X}(t)$.

A. **Path-loss model**

A large number of empirically-derived propagation models are available in the literature for both the sub-6 GHz band and the unlicensed ISM millimeter wave (mmW) band around 60 GHz, providing the expected power path-loss (PL) vs. the TX-RX distance d. Most of them are in the following form [13]

$$\overline{PL}(d)\big|_{\text{dB}} = \overbrace{10 \cdot \gamma \cdot \log_{10}(d / d_0) + PL(d_0)\big|_{\text{dB}}}^{PL(d)} + \Xi\big|_{\text{dB}} \tag{1}$$

where γ is the PL exponent (PLE), d_0 is the minimum TX-RX separation for which the model is valid, and $\Xi\big|_{\text{dB}}$ is a zero-mean Gaussian random variable (RV), with standard deviation $\sigma_{\Xi}\big|_{\text{dB}}$, which takes into account for the long term fading caused by the shadowing phenomenon. In this paper we will use the experimentally-derived parameters for both line-of-sight (LOS) and non-LOS (NLOS) industrial/office indoor propagation, listed in Table 2; parameters for sub-6 GHz band are derived from [13], while parameters for the 60 GHz band are derived from [14]. Also, that the value of $PL(d_0)$ can be either derived from experimental measures, or theoretically evaluated by assuming free-space (FS) propagation from the antenna to the boundary of the validity region of the path-loss model, at distance d_0 from the transmitter.

Table 2: Parameters for indoor path loss models in sub-6 GHz and 60 GHz bands

Frequency Band	Ref.	Propagation conditions	PL model parameters			
			γ	d_0	$PL(d_0)\big\|_{\text{dB}}$	$\sigma_{\Xi}\big\|_{\text{dB}}$
sub-6 GHz	[13]	LOS	1.25 – 2.68	15 m	Empirical 57.67 – 77.57 dB Free-Space < 71.52 dB	4.32 – 5.74 dB
		NLOS	0.68 – 4.47	15 m	Empirical 64.42 – 83.33 dB Free-Space < 71.52 dB	3.16 – 8.42 dB
60 GHz	[14]	LOS	0.5 – 2.5	1 m	Empirical 34 – 84 dB Free-Space 68 dB	0.14 – 5.4 dB
		NLOS	1.64 – 5.4	1 m	Empirical 35 – 86 dB Free-Space 68 dB	1.55 – 8.6 dB

B. **Multipath channel model**

We assume a multipath channel model, whose BBCR consists of $M+1$ paths, and each path introduces a propagation delay τ_m and a random complex-valued gain $\tilde{A}_m$ ($0 \le m \le M$). Denoting with $m = 0$ the path carrying the useful signal, without loss of generality we assume $\tau_0 = 0$. The multiplicative coefficients $\tilde{A}_m$ of the multipath channel are modelled as independent and identically distributed (i.i.d.) complex-valued random variables (RVs), with Rayleigh amplitude and uniform phase, which are the responsible for the short-term fading and are suitably scaled such that $\sum_{m=0}^{M} \mathrm{E}\{|\tilde{A}_m|^2\} \equiv 1$, where $\mathrm{E}\{\cdot\}$ denotes statistical expectation.

C. **Signal model**

According to the propagation model outlined in Sect. 3-B the BBCR of the RF signal $R(t)$ at RX side is

$$\tilde{R}(t) \equiv \overbrace{\sqrt{\Gamma}\tilde{A}_0\tilde{S}(t)}^{\tilde{U}(t)} + \overbrace{\sqrt{\Gamma}\sum_{m=1}^{M}\tilde{A}_m \cdot \tilde{S}(t-\tau_m)}^{\tilde{I}(t)} + \tilde{N}(t) \tag{2}$$

where: $\Gamma \equiv G_{\text{t}}G_{\text{r}} / \overline{PL}(d)$ is the power gain of the link, with G_{t} and G_{r} representing TX and RX antenna gains, respectively; $\tilde{S}(t)$ is the BBCR of the RF signal $S(t)$ fed to the TX antenna, whose RF power is P_S; $\tilde{U}(t)$ is the BBCR of the RF useful signal $U(t)$ (including the Rayleigh fading coefficient $\tilde{A}_0$), whose RF power is $P_U \equiv \Gamma\,\mathrm{E}\{|\tilde{A}_0|^2\}\,P_S$; $\tilde{I}(t)$ is the BBCR of the RF multipath interfering component $I(t)$, whose RF power is $P_I \equiv \Gamma\sum_{m=1}^{M}\mathrm{E}\{|\tilde{A}_m|^2\}\,P_S$; $\tilde{N}(t)$ is the BBCR of the overall additive white Gaussian noise (AWGN) process $N(t)$.

The amount of the multipath components is quantified by the "useful-to-multipath power ratio"(also known as Rice factor) defined as [15]

$$K \equiv \frac{P_U}{P_I} = \frac{\mathrm{E}\{|\tilde{A}_0|^2\}}{\sum_{m=1}^{M}\mathrm{E}\{|\tilde{A}_m|^2\}} = \frac{\mathrm{E}\{|\tilde{A}_0|^2\}}{1-\mathrm{E}\{|\tilde{A}_0|^2\}} \tag{3}$$

In the case of sub-6 GHz links, experimental values for K are found in the range 3.5 – 18.6 dB [13], while for 60 GHz links they are shown to lie in the ranges 0.89 – 7.31 dB and 5 – 15 dB [15, 16]. From (3), we get $\mathrm{E}\{|\tilde{A}_0|^2\} = K/(K+1)$, and the RF power of the useful signal can be expressed as in Eq. (4).

$$P_U = \frac{\left(\frac{K}{1+K}\right) P_S \, G_\mathrm{t} \, G_\mathrm{r}}{\overline{PL}(d)} \tag{4}$$

Concerning data transmission, the selected modulation and coding scheme (MCS) consists of a modulation with constellation size W and an error-correcting code with rate r. The bit rate is $R_b \equiv 1/T_b$, where T_b is the bit interval, and the symbol rate is $R_s \equiv 1/T_s$, where T_s is the symbol interval, with $R_b = R_s \, r \log_2 W$. The average useful received RF energy during one bit and one symbol interval are thus $E_b \equiv P_U / R_b$ and $E_s \equiv P_U / R_s$, respectively, with $E_b = E_s / (r \log_2 W)$.

D. **Noise model**

$\tilde{N}(t)$ is the BBCR of the overall AWGN process $N(t)$ and it includes both channel and RX noise contributions. The one-sided RF PSD of *N(t)* is $\eta_0^{(N)} \equiv \mathrm{k}[T_A + (F-1)T_0]$, where $\mathrm{k} = 1.38 \cdot 10^{-23}$ J / K is the Boltzmann's constant, T_A is the noise temperature of the RX antenna and F is the noise figure of the RX front-end referred to the reference temperature $T_0 = 290$ K. The (atmospheric, cosmic and ground-originated) noise picked up by the antenna is negligible; hence we let $T_A = 0$ K and $\eta_0^{(N)} = \mathrm{k}(F-1)T_0$. The RF power P_N of the Gaussian noise is $P_N \equiv \eta_0^{(N)} B_N$, where B_N is the one-sided RF noise bandwidth. Assuming Root Raised-Cosine (RRC) pulse shaping, we get $B_N = R_s$. Furthermore, assuming a large number of i.i.d. components ($M >> 1$), the RF multipath term $I(t)$ can be modelled as a Gaussian process with zero mean, variance P_I, and one-sided RF PSD $\eta_0^{(I)} \equiv P_I / B_N$, so that the PSD of the overall Gaussian noise can be expressed as $\eta_0 \equiv \eta_0^{(N)} + \eta_0^{(I)}$.

E. **Performance metrics and link design**

The performance metrics considered in this work are: *i*) the maximum required value of the bit error rate (BER) at the RX side p_b, denoted as p_req; *ii*) the outage probability, defined as $p_\mathrm{out} \equiv \Pr\{p_b > p_\mathrm{req}\}$.

The link design must thus ensure that $p_b \le p_\mathrm{max}$ at the RX side, and such a requirement translates in the equivalent condition $E_b / \eta_0 \ge (E_b / \eta_0)_\mathrm{req}$, where $(E_b / \eta_0)_\mathrm{req}$ is the value of E_b / η_0 yielding a BER lower than p_max. With some simple algebra and letting $\overline{PL}(d) = PL(d)\,\Xi$, the E_b / η_0 ratio can be re-written as

$$\frac{E_b}{\eta_0} = \frac{K}{\frac{(K+1)\, PL(d)\, \Xi\, \eta_0^{(N)}\, R_b}{P_S \, G_\mathrm{t} \, G_\mathrm{r}} + r \log_2 W} \ge \left(\frac{E_b}{\eta_0}\right)_\mathrm{req} \tag{5}$$

and with some further manipulation, we get the following expression, where we introduced the threshold ξ (also termed fading margin)

$$\Xi \le \xi \equiv \frac{P_S \, G_\mathrm{t} \, G_\mathrm{r}}{(K+1)\, PL(d)\, \eta_0^{(N)}\, R_b} \left(\frac{K}{(E_b / \eta_0)_\mathrm{req}} - r \log_2 W \right) \tag{6}$$

The random attenuation Ξ can exceed the threshold ξ, thus violating the above inequality, and causing an outage event, whose probability can be written as $p_\mathrm{out} = \Pr\{\Xi > \xi\}$. Recalling that the logarithmic attenuation $\Xi|_\mathrm{dB}$ is a zero-mean Gaussian RV with standard deviation $\sigma_{\Xi}|_\mathrm{dB}$, the outage probability turns out $\mathrm{Q}(x)$, where $p_\mathrm{out} = \mathrm{Q}(\xi|_\mathrm{dB} / \sigma_{\Xi}|_\mathrm{dB})$ is the Gauss' integral function. The link-budget equation for the assessment of the sustainable bit rate R_b vs. the link distance d, is derived by putting (6) in logarithmic form, as shown hereafter

$$R_b|_\mathrm{dBHz} = P_S|_\mathrm{dBm} + G_\mathrm{t}|_\mathrm{dBi} + G_\mathrm{r}|_\mathrm{dBi} - 10\log_{10}(K+1) - PL(d)|_\mathrm{dB} - \eta_0^{(N)}|_\mathrm{dBm/Hz} - \xi|_\mathrm{dB} + 10\log_{10}\left(\frac{K}{(E_b / \eta_0)_\mathrm{req}} - r \log_2 W \right) \tag{7}$$

From (5), it is also apparent that, due to the presence of the multipath component, the E_b / η_0 ratio reaches a floor when the AWGN contribution vanishes

$$\lim_{\eta_0^{(N)} \to 0} \frac{E_b}{\eta_0} = \frac{K}{r \log_2 W} \tag{8}$$

so that the requirement $E_b / \eta_0 \geq (E_b / \eta_0)_{\text{req}}$ is fulfilled only if K is greater than K_{min}, as defined in the following

$$K\big|_{\text{dB}} \geq K_{\min}\big|_{\text{dB}} \equiv 10 \log_{10}(r \log_2 W) + \left(\frac{E_b}{\eta_0}\right)_{\text{req}}\Bigg|_{\text{dB}} \tag{9}$$

4. H²AWKS SIMULATION RESULTS

The numerical values of the system parameters that have been adopted for an example of link analysis in the sub-6 GHz band are listed in Table 3, whereas the following values of the propagation models have been selected from those reported in Table 2.: *i*) for the LOS case $\gamma = 2.68$, $PL(d_0) = 77.57$ dB, and $\sigma_{\Xi}\big|_{\text{dB}} = 5.74$ dB; *ii*) for the NLOS case $\gamma = 4.47$, $PL(d_0) = 83.33$ dB, and $\sigma_{\Xi}\big|_{\text{dB}} = 8.42$ dB. Concerning the MCS, for the sake of simplicity, we focused on single-carrier transmissions employing Quadrature Phase Shift Keying (QPSK) modulation, with customary concatenated Reed-Solomon (RS) and convolutional encoding for error-correction [17][1], which also complies with the requirement (9).

Table 3: Numerical values of the link-budget parameters for sub-6 GHz band

Parameter description	Symbol	Value or value range
Transmitter power	$P_S\big\|_{\text{dBm}}$	10 dBm
Transmitter and receiver antenna gains	$G_{\text{t}}\big\|_{\text{dBi}}$, $G_{\text{r}}\big\|_{\text{dBi}}$	12 dBi, 1.4 dBi
Noise figure of the receiver RF front-end	$F\big\|_{\text{dB}}$	5 – 10 dB
Bit rate of the data link	R_b	1 kb/s to 10 Mb/s
Useful-to-multipath power ratio (Rice factor) of the propagation channel model	$K\big\|_{\text{dB}}$	7 – 14 dB
Size of the digital modulation constellation	W	4
Rate of the error-correcting code	r	$\frac{1}{2} \cdot \frac{188}{204}$
Required "energy per bit-to-noise density" ratio yielding an error rate lower than p_{req}	$(E_b / \eta_0)_{\text{req}}\big\|_{\text{dB}}$	5.5 dB
Maximum tolerable bit error rate	p_{req}	$<10^{-10}$
Outage probability	p_{out}	$2.28 \cdot 10^{-2}$
Fading margin	$\xi\big\|_{\text{dB}}$	11.48 – 16.84 dB

As apparent from (9), the choice of the MCS reveals a critical issue in the design of the radio link and as such it rules out the utilization of low energy-efficiency schemes, i.e., having high values of $(E_b / \eta_0)_{\text{req}}$, in propagation environments heavily affected by multipath, i.e., in the presence of low values of the Rice factor K. Furthermore, by designing the link with a fading margin $\xi\big|_{\text{dB}} = 2\sigma_{\Xi}\big|_{\text{dB}}$ (i.e., from 11.48 to 16.84 dB), the outage probability results $p_{\text{out}} = \text{Q}(2) \approx 2\%$, which could represent a good trade-off between the efficient use of the limited TX power and the link reliability. Hereafter, Figs. 1 and 2 show the results of a wireless link analysis, simulated with the models in Sections 2 and 3. With reference to the data in Table 3, Fig. 1 and 2 show the achievable bit-rate as a function of connection

[1] The performance of the MCS scheme has been excerpted from Fig. 4 of [17] and assumes a Rayleigh fading affecting the main signal path, plus additional self-interference arising from scattered/delayed multipath components.

distance, in both LOS and NLOS scenarios. In detail. the curves in Fig. 1 refers to different values of RX noise figure F (5 and 10 dB) while Fig. 2 refers to different values of the useful-to-multipath power ratio K (7 and 14 dB). Figure 3 presents the control panel of the H2AWKS radio link design software, developed using National Instruments' LabVIEW development environment.

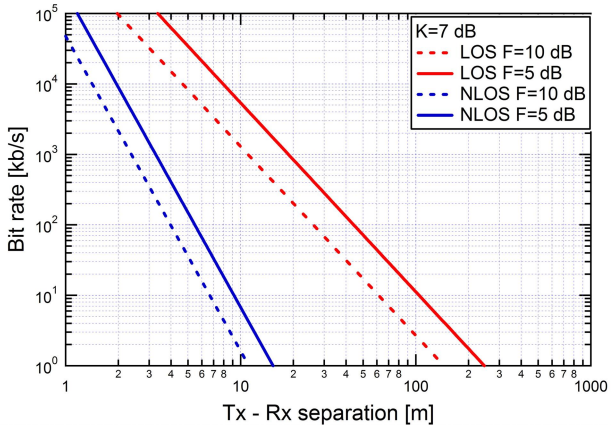

Figure 1. Bit-rate vs. link distance, with the receiver noise figure F as the parameter (LOS and NLOS scenarios).

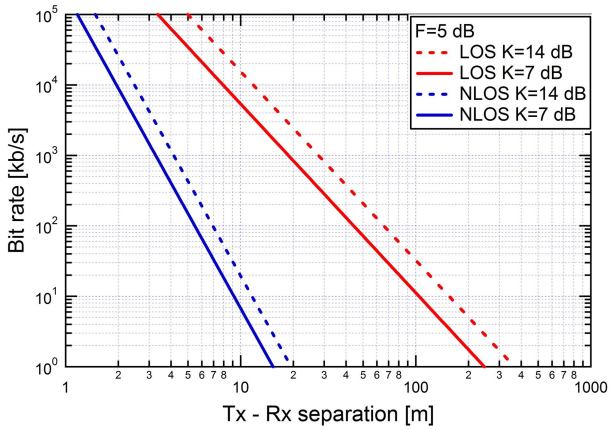

Figure 2. Bit-rate vs. link distance, with the useful-to-multipath power ratio K as the parameter (LOS and NLOS scenarios).

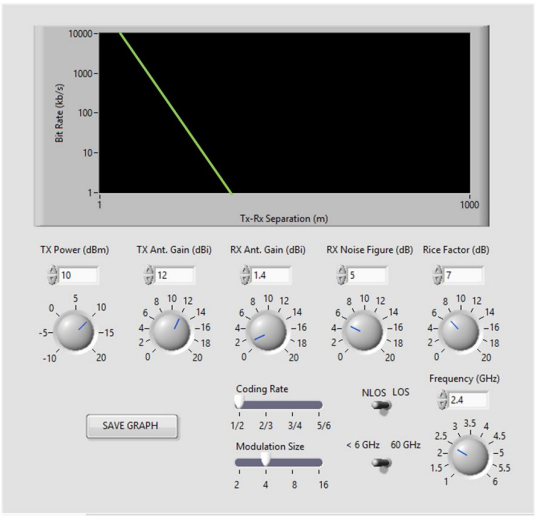

Figure 3. Control panel of the H^{2}AWKS radio link design software, developed with National Instruments' LabVIEW.

5. CONCLUSIONS

The paper presented the development of H^{2}AWKS (Harsh environment and Hardware Aware Wireless linK Simulator), a simulator that allows planning a WSAN taking into account environment constraints and hardware parameters. The equations that are at the core of H^{2}AWKS, as well as its application in a real case, are shown. H^{2}AWKS is useful for the design exploration of the system performance of a WSAN as a function of the operating environment and of the hardware parameters of the used devices. For instance, as shown in Sect. 4, H^{2}AWKS allowed the design exploration of a wireless link in realistic multipath environment, including COTS device specifications, varying the parameters of the radio propagation channel model and deriving the link performance constraint in terms of bit rate vs. link distance relationship. This way, thanks to H^{2}AWKS the developers of Internet-of-Things (IoT) solutions can exploit the large offer of COTS devices at the state of art: single-chip solutions embedding in the same device a microcontroller core with a wireless transceiver which support different protocols (Bluetooth, ZigBee, Bluetooth Low Energy, sub- GHz links), from about 300 MHz to 6 GHz, and some of them also enabling mmW clinks at 60 GHz.

REFERENCES

[1] K.F. Tsang et al., “Industrial wireless networks: applications, challenges, and future directions,” IEEE T. Ind. Inf., 12 (2), 755-775 (2016)

[2] L. Ascorti et al., “A wireless cloud network platform for critical data publishing in industrial process automation,” IEEE Sensors Application Symposium, 1-6 (2016)

[3] ChenYang Lu, "Real-Time Wireless Control Networks for Cyber-Physical Systems", IEEE INFOCOM (2014)

[4] M. Boers et al., "A 16TX/16 RX A 16TX/16RX 60GHz 802.11ad chipset with single coaxial interface and polarization diversity", IEEE ISSCC Conference, 344-345 (2014)

[5] TI, “CC2592 2.4-GHz Range Extender”, pp. 1-14, SWRS159 (2014)

[6] M. Chakravarti et al., “RF multi-function chip at Ku-band”, IEEE IMARC (2015)

[7] TI, “CC3100 SimpleLink Wi-Fi Network Processor, Internet-of-Things Solution for MCU Applications”, SWAS031D, pp. 1-44, (2015)

[8] TI, “CC256x Dual-Mode Bluetooth Controller”, SWRS121E, pp. 1-46, (2016)

[9] TI, “CC1310 SimpleLink™ Ultra-Low-Power Sub-1 GHz Wireless MCU”, SWRS181C, pp. 1-59 (2016)

[10] Semtech, “SX1276/77/78/79 - 137 MHz to 1020 MHz Low Power Long Range Transceiver”, Rev. 4, pp. 1-132 (2015)

[11] https://www.maximintegrated.com/en/datasheet/index.mvp/id/4191HMC63xx

[12] HMC6301, “Millimeterwave Receiver, 57 GHz to 64 GHz”, v00.0716, (2016)

[13] E. Tanghe, W. Joseph, L. Verloock, L. Martens, H. Capoen, K. Van Herwegen, W. Vantomme, " The Industrial Indoor Channel: Large-Scale and Temporal Fading at 900, 2400, and 5200 MHz," IEEE Transactions on Wireless Communications, 7 (7), 2740-2751, (2008)

[14] C. Gustafson, *60 GHz wireless propagation channels: characterization, modeling and evaluation*, Ph.D. Thesis, Department of Electrical and Information Technology, Lund University, Lund, Sweden, (2014).

[15] H.-X. Zheng, “A model of 60 GHz indoor radio channel,” Int. Journal of Infrared and Millimeter Waves, 24 (11), 1861-1873, (2003).

[16] D. Dardari, et al., "Wideband indoor communication channels at 60 GHz," IEEE PIMRC'96, vol. 3, 791–794 (1996).

[17] Digital Video Broadcasting; Implementation guidelines for DVB terrestrial services; Transmission aspects, ETSITR101190 V1.1.1 (1997-12).